

## Dry Sliding Wear Behavior and Evaluation of Mechanical Properties of AA6061-B<sub>4</sub>C Composites

D. P. Bhujanga<sup>1</sup>, H. R. Manohara<sup>2</sup>

<sup>1</sup>Department of Mechanical Engineering, SDM Institute of Technology, Ujire-574240, Karnataka, India.

<sup>2</sup>Department of Mechanical Engineering, SJM Institute of Technology, Chitradurga-577502, Karnataka, India.

**ABSTRACT :** The Paper reports a study on the processing and evaluation of Wear behavior and mechanical properties of AA6061 alloy reinforced with B<sub>4</sub>C particulates of having average particle size of 220 μm with varying weight percentage of 1%, 2%, 3% & 4% by liquid metallurgical route. Bi potassium hexa fluoro titanate (K<sub>2</sub>TiF<sub>6</sub>) flux is added to incorporate boron carbide into aluminium melt and to enhance better wettability of B<sub>4</sub>C particles in the matrix. To study the microstructure of the prepared composites scanning electron microscope (SEM) equipped with an energy dispersive X- ray analysis (EDAX) were used. SEM micrographs reveal the homogeneous dispersion of B<sub>4</sub>C particles in the matrix. The reinforcement dispersion has also been identified with X-ray diffraction (XRD). The wear properties of the samples were studied using pin-on disk apparatus. Worn surface were characterized by SEM to understand the wear mechanism exhibited by the prepared composites. The results indicates that adding B<sub>4</sub>C particulates in AA6061 matrix increases the Wear resistance, hardness and ultimate tensile strength.

**Keywords -** AA6061, B<sub>4</sub>C, EDAX, SEM, XRD.

### I. INTRODUCTION

The importance of composites as engineering materials is reflected by the fact that out of over 1600 engineering materials available in the market today more than 200 are composites because of their excellent behaviour with their high strength to weight ratio. Conventional monolithic materials have limitations with respect to achievable combinations of strength, stiffness, and density. In order to overcome these shortcomings and to meet the ever increasing engineering demands of modern technology, metal matrix composites are gaining importance [1, 5].

Aluminium matrix composites (AMMCs) are attractive and competent materials for military, marine, space, nuclear, automotive and aircraft industries because of its excellent tribological and mechanical properties. Due to vast market needs there is huge interest and demand in research and development on aluminium metal matrix composites.

In AMMCs, the major constituent is aluminium alloy, which acts as the matrix phase. The other constituent embedded in the aluminium alloy matrix which serves as reinforcement are usually non-metallic, and commonly include ceramics such as silicon carbide, aluminium oxide etc.

The major advantages of AMMCs compared to unreinforced materials are greater strength, improved stiffness, reduced weight, improved high temperature properties, controlled

thermal expansion coefficient, thermal/heat management, enhanced and tailored electrical performance, improved abrasion and wear resistance as well as improved damping capabilities [5, 10]. Properties of AMMCs can be tailored by varying the type, size of constituents and percentage of reinforcement.

Particulate Reinforced Aluminium Metal Matrix Composites are much less expensive to fabricate than continuously reinforced composites. Consequently, performance enhancement of the matrix comes at lower additional costs in comparison to composites with aligned reinforcements. Silicon carbide, alumina, boron carbide, and graphite are common reinforcements for aluminium matrices [10, 16].

Boron carbide is the third hardest material after diamond and cubic boron nitride, which possesses low density (2.51 g/cm<sup>3</sup>), high hardness (3700 N/mm<sup>2</sup>), high stiffness (445 Gpa), high specific strength, high strength, high shock resistance, high wear and impact resistance, high toughness, has a relatively low fracture toughness, low specific weight, low specific gravity [17, 20]. Boron carbide has high melting point (2450 °C) as well as high resistance to chemical agents. It is an attractive strengthening agent for aluminium-based composites. One of the special features of boron carbide is that the ability to absorb neutron is considerably high. These features allowed boron carbide to be applied in nuclear industry as neutron absorber materials. Aluminium reinforced boron

carbide composite gives interesting features such as high strength and high hardness, good tribological properties due to presence of hard reinforcements. These characteristics have made this composite as a very potential material in engineering field. Fabrication of aluminium composite reinforced with boron carbide is difficult due to several weaknesses of boron carbide when it exists as a single form where boron carbide is brittle and required extreme temperature for heat treatment due to its high melting point [20, 25]. By using boron carbide as the reinforcement and metal as matrix to produce metal matrix composite, the problem related to the brittleness can be solved. Until now, metal often been used is aluminium because of its characteristics that are light in weight and have the ability to wet the boron carbide at high temperature [26]. It could be an alternative to silicon carbide composites in applications where high stiffness and wear resistance are major requirements. One of the solutions is going for boron carbide reinforced metal matrix composites that are stronger, stiffer, fracture resistant, lighter in weight, harder, possess higher fatigue strength and exhibit significant improvements over other materials [26]. The lower density, high elastic modulus, high refractoriness and higher hardness of B<sub>4</sub>C than SiC and Al<sub>2</sub>O<sub>3</sub> make it better reinforcement for high performance MMCs. It has been reported that the interfacial bonding between the aluminium matrix and the B<sub>4</sub>C reinforcement seems to be better than that between aluminium matrix and SiC. However, a limited research work has been reported on AMCs reinforced with B<sub>4</sub>C due to poor wetting and higher raw material cost [26, 30].

## II. EXPERIMENTAL DETAILS

### 2.1 Material Selection

In the present work matrix used is AA6061.

Table 1. Gives the chemical composition of AA6061.

**TABLE 1** Chemical Composition of AA6061

| Mg   | Si   | Fe   | Cu   | Mn   | Cr   | Zn   | Ti   | Al      |
|------|------|------|------|------|------|------|------|---------|
| 0.95 | 0.54 | 0.22 | 0.17 | 0.13 | 0.09 | 0.08 | 0.01 | Balance |

Boron carbide (B<sub>4</sub>C) of particle size 220 mesh size is chosen as reinforcement material. Table 2. Gives the properties of B<sub>4</sub>C.

**TABLE 2** Properties of B<sub>4</sub>C

| Density (g/cm <sup>3</sup> ) | Melting Point (°C) | Hardness (Gpa) | Young's Modulus (Gpa) | Stiffness (Gpa) |
|------------------------------|--------------------|----------------|-----------------------|-----------------|
| 2.52                         | 2880               | 30             | 540                   | 445             |

### 2.2 Fabrication process

The proposed AMCs were prepared by the liquid metallurgy route in an induction heating furnace. To improve wettability between B<sub>4</sub>C with Al matrix K<sub>2</sub>TiF<sub>6</sub> halide salt (Potassium Titanium fluoride) is added as a flux to the melt. At an appropriate Ti level, the Titanium rich reaction layer covers the B<sub>4</sub>C particulates and thus these particles are wetted by Al melt. The titanium rich layer consists of particle clusters of Titanium carbide and Titanium di-boride formed on the B<sub>4</sub>C surface. K<sub>2</sub>TiF<sub>6</sub> incorporate B<sub>4</sub>C particulates in the melt and improves wettability of B<sub>4</sub>C particle with molten aluminium. This reaction is exothermic in nature and heat evolved in the vicinity of B<sub>4</sub>C particle-melt interface. The local increase in temperature enhance the incorporation of particles in to the melt and bonding with the matrix. Also magnesium present in AA6061 alloy is also found to increase the wettability of the particulates by reducing the surface tension of the melt.

### 2.3 Preparation of cast composites

A batch of 250g of AA6061 was melted at 760°C in a graphite crucible using in a high frequency induction furnace. The melt was agitated with the help of a zirconia coated steel rod to form a fine vortex. Degassing tablet (C<sub>2</sub>Cl<sub>6</sub>-Solid hexachloro ethane) was added to the vortex and slag was removed from the molten metal. Degasser remove all the absorbed gases in the melt. Once the temperature reaches 810°C the preheated mixture of B<sub>4</sub>C (200 °C for 1 hour) with an equivalent amount of K<sub>2</sub>TiF<sub>6</sub> halide salt (with 0.05 Ti/ B<sub>4</sub>C ratio) were added by packed in an aluminium foil into the vortex. Before pouring the molten metal to the mould the melt held at 5 min as holding time with cover flux (45% NaCl + 45% KCl + 10% NaF). Cover flux helps in decreased contact angle and surface tension forces. The molten metal at a temperature of 860 °C, then poured into the preheated graphite mould. The cast samples were of 12.5 mm diameter, 125 mm length. The AMCs having particle size of 220 mesh with varying weight percentage of 0%, 1%, 2%, 3% and 4% of B<sub>4</sub>C were fabricated by the same procedure.

### 2.4 Microstructure and testing

Microstructure characterization of the prepared composites was carried out using scanning electron microscope (SEM). The specimens were cut and prepared as per standard metallographic procedure. The specimen were prepared by grinding through 400, 600, 800 and 1000 mesh emery papers. Polishing is done for the specimen to get fine surface

finish. Specimens were then etched using Keller's reagent ( $\text{HNO}_3+\text{HCL}+\text{HF}+\text{H}_2\text{O}$ ).

The micrographs of etched specimen were observed using the scanning electron microscope (SEM). The energy dispersive X-ray analysis (EDAX) was carried out on the prepared composites to reveal the presence of reinforcement in the matrix. X-ray diffractions (XRD) was also used for identifying the presence of  $\text{B}_4\text{C}$  particles and to study the interface characteristics. The hardness was measured at different location at room temperature using micro Vickers hardness tester. Specimens of dimensions 10 mm length and 12mm diameter were polished using metallographic procedure till mirror finish on surface is obtained. The microhardness of polished specimens was measured using micro-vicker hardness tester at a load of 200 g for 10 sec. The hardness measurement was carried out at 20 different locations & average of readings were recorded. The tensile specimens were prepared as per ASTM E8 standard. The ultimate tensile strength (UTS) was evaluated using a computerized universal Testing Machine.

The Dry sliding wear test in this research work is performed according to ASTM G99 standard. The test were conducted on computerized Pin-on-Disc wear- testing machine (DUCOM TR-20-PHM 400). The pins used were produced from the extruded samples in the shape of cylinder with diameter 10mm and height 20mm and it was held against the counter face of the rotating disc with wear track diameter 90mm. The wear test was performed by loading the pin against the disc through a dead weight loading system. In order to ensure perfect contact of flat surface of the specimen with the steel disc, the surface of the pin samples were slide using emery papers of different grit size. Before and after each test, the pins and wear track are cleaned with acetone and then pins are weighed carefully and weight losses are recorded. Dry sliding wear test at sliding speed of 0.9 m/s and with imposing load of 20 N to 60 N for a sliding distance of 282.7 m were carried out on the pin specimens at room temperature.

### III. RESULTS AND DISCUSSIONS

#### 3.1 Microstructural analysis

The aluminium reinforced with  $\text{B}_4\text{C}$  particulate composites are successfully processed by liquid metallurgical routes. The experimental results shows two important aspects: 1. Uniform distribution of  $\text{B}_4\text{C}$  particulates in the composites. 2. Good wettability between  $\text{B}_4\text{C}$  and AA6061. The wettability Problem associated with the  $\text{B}_4\text{C}$  particle with molten aluminium has been resolved by the incorporation of  $\text{K}_2\text{TiF}_6$  flux. The  $\text{K}_2\text{TiF}_6$  flux

facilitates the incorporation of  $\text{B}_4\text{C}$  particle in to the aluminium melt. On the melted surface of  $\text{B}_4\text{C}$  particulates flux reacts and produces Ti compounds around it. The nature of the above reaction is exothermic and heat evolved melt the interface, also the increase in the local temperature accelerates the incorporation of  $\text{B}_4\text{C}$  particulates in to the aluminium melt and enhances bonding with the matrix.

The presence of Ti in the form of  $\text{K}_2\text{TiF}_6$  halide salt contributes towards removal of the oxide layer from aluminium melt there by improving the wettability. Fig. 4 shows scanning electron micrograph (SEM) of fabricated AMCs with varying weight percentage of  $\text{B}_4\text{C}$ . The SEM images reveal that the uniform distribution of  $\text{B}_4\text{C}$  particles in the aluminium matrix for all wt%. This is due to effective stirring action and selection of appropriate process parameters during casting and also due to the equal value of density of matrix and reinforcement material causing the particle neither float nor descent in the mixture. Hence the particles are segregated at the inter dendrite region. The Ti compound reaction layer was formed when adding  $\text{K}_2\text{TiF}_6$  halide salt flux into the melt where K and F contributed for removing of the oxide film from the Al surface. The weak reaction layer in the region was not so clear in the SEM image due to the removal of interfacial reaction layer during polishing.

Fig. 5 reveals the presence of rich white layer of Ti compound. However in some region the weak Ti compound layer is also observed. The magnified image clearly highlight the interface between the matrix and particulate reinforcement. The layers consisting of titanium boride and titanium carbide having different shapes is grown over  $\text{B}_4\text{C}$  particles. Presence of this rich Ti layer around  $\text{B}_4\text{C}$  particles improves wettability and interfacial bonding between matrix and reinforcement.

#### 3.2 EDAX and XRD analysis

The energy dispersive X-ray analysis (EDAX) was carried out on the AA6061-4%  $\text{B}_4\text{C}$  composites. Fig. 6 (a) shows the EDAX pattern which reveals the presence of reinforcement in the matrix. XRD analysis is presented in Fig. 6 (b) it is evident from the XRD pattern that the  $\text{B}_4\text{C}$  particles did not react with Al matrix and produced any other compounds used. In this present work at synthesizing temperature,  $\text{B}_4\text{C}$  particles are thermodynamically stable. This is due to formation of Ti compound layer around the  $\text{B}_4\text{C}$  particles which tends to react as a reaction barrier and prevents the interfacial reactions between aluminium matrix and  $\text{B}_4\text{C}$ .

### 3.3 Evaluation of mechanical properties

#### 3.3.1 Microhardness

Fig. 1 shows the micro Vicker hardness of the cast specimens with different particulate weight fraction.

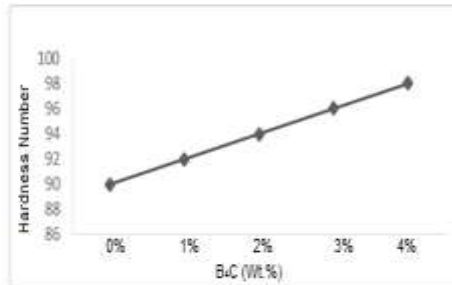


Fig. 1 The effect of wt. % of B<sub>4</sub>C particulates on the hardness

It is observed that the micro hardness of the AMCs are increased with increasing the wt% of B<sub>4</sub>C reinforcement. The micro Vickers hardness value of the AMCs was found to maximum (100 VHN) for 4% reinforcement and there is appreciable increase in hardness value compare to the ascast. The presence of such hard surface area of particles offer more resistance to plastic deformation which leads to increase in the hardness of composites.

Addition of reinforcement particles in the matrix increases the surface area of the reinforcement and the matrix grain sizes are reduced. Also the addition of reinforcement particles in the melt provides additional substrate for the solidification to trigger there by increasing the nucleation rate and decreasing the grain size.

#### 3.3.2 Tensile strength

Fig. 2 shows the relation between ultimate tensile strength of AMC's and the weight % of B<sub>4</sub>C particulates. The tensile strength of the AMCs was tested using computerized universal testing machine. The tensile specimens were prepared as per ASTM E8 standard.

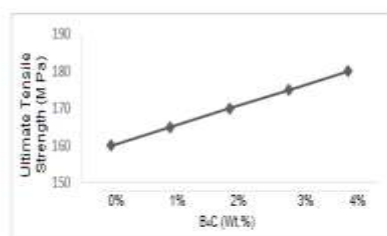


Fig. 2 The effect wt. % of B<sub>4</sub>C particulates on the ultimate tensile strength

It is observed that tensile strength is increased with increasing the wt% B<sub>4</sub>C reinforcement. The tensile strength of the AMCs

was found to maximum for 4% reinforcement. The ultimate tensile strength of composites has increased from 160 MPa to 180 MPa. This is due to effective transfer of applied tensile load to the uniformly distributed well bonded particulate reinforcement in the matrix. The addition of B<sub>4</sub>C particles in the matrix to the increase in hardness of composite. A strong bonding between reinforcement and aluminium matrix favors the enhancement of ultimate tensile strength of the composite gives much strength to AA6061 matrix alloy by offering more resistance to tensile stresses.

The Increase in the strength is due to the increase in hardness of composite. A strong bonding between reinforcement and aluminium matrix favors the enhancement of ultimate tensile strength of the composite.

#### 3.4 Worn surface studies

Worn surface studies were carried out using scanning electron microscope and presented in Fig. 7. All the worn out surface are at constant sliding speed of 0.9m/s and constant sliding distance of 282.7 m under ambient conditions. There is formation of oxide layer on the surface which avoids establishing of direct contact between aluminium alloy and disc, resulting in decrease of wear rate. Oxide layer acts as a tribological layer which is formed due to presence of considerable amount of oxygen and iron on the surface. Micrographs also reveals the fine long continuous parallel abrasive grooves running throughout the surface, this indicates the mild abrasive wear is predominant. Also there is a presence of fine discontinuous parallel groves with oxide layer indicating mild wear. Worn surface clearly shows the crack formation indicating severe wear. As the load increases there is clear visibility of fine groves with more depth which indicates the transition from mild wear normal wear to and then normal wear to severe wear. Poor wear track is due to uniform distribution of AA6061 matrix which makes surface harder and material removal takes place due to sub surface layer.

#### 3.5 Wear behavior

Wear properties of the prepared composites were studied using pin-on disc wear testing machine under ambient test conditions. Fig. 3 shows wear rate v/s load at constant sliding speed and constant sliding distance. Wear rate decreases as the load increase and it is found minimum for AA6061-4% B<sub>4</sub>C composites. The lower wear rate is due to presence of hard ceramic particulate B<sub>4</sub>C particulates in ductile Al matrix, which prevents direct contact



between metal to metal contact and also due to formation of more tribolayers.

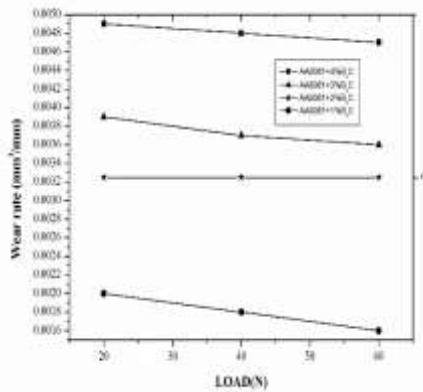


**Fig. 3** Wear rate v/s Load at constant sliding speed and constant sliding distance.

#### IV. CONCLUSION

The AA6061-B<sub>4</sub>C composites was successfully produced by liquid metallurgical routes with different weight percentage (viz., 1, 2, 3 and 4) of reinforcement and the microstructure, mechanical and tribological properties are evaluated. The following conclusions are derived from the study.

- Scanning electron Photomicrographs (SEM), EDAX and XRD analysis revealed the presence of

B<sub>4</sub>C particles in the composites with homogeneous dispersion.

- The K<sub>2</sub>TiF<sub>6</sub> halide salt (Potassium Titanium fluoride) flux is the most attractive route for the processing of AA60601-B<sub>4</sub>C discontinuously reinforced composites (DRA).

- Thin Titanium rich interfacial reaction layer is responsible for the incorporation of B<sub>4</sub>C particulates in Aluminium matrix.

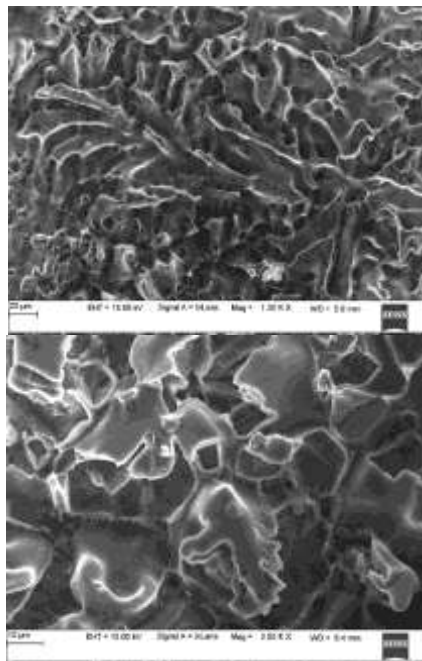
- The increase in the weight percentage of reinforcement led to increase in the microhardness level and found maximum (98 VHN) for 4 wt%.

- The ultimate tensile strength of composites has increased from 160 MPa to 180 MPa and was found maximum for 4 wt%.

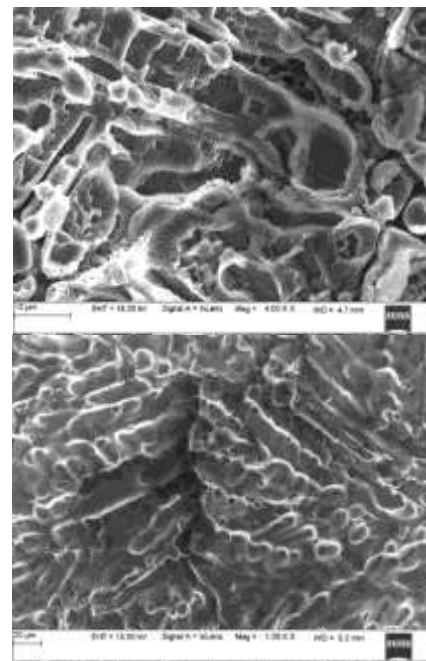
- Wear resistance capability of composites increases with increase in wt. % of reinforcement and it is significantly improved due to successful integration of hard ceramic B<sub>4</sub>C particulates on ductile AA6061 matrix.

- Worn out surfaces reveal the transition of mild to normal wear, normal wear to severe wear, as a result of increase in the load.

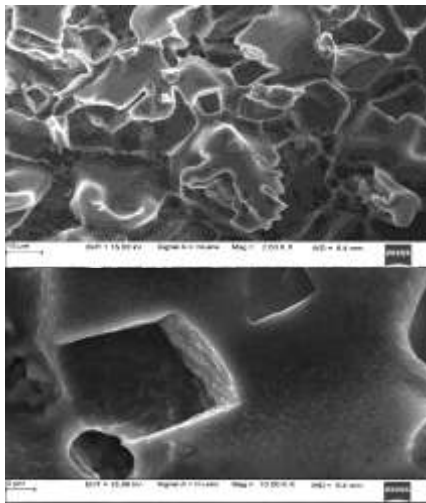
- SEM Photomicrographs of Worn surfaces also reveals different wear mechanisms such as delaminative wear, adhesive wear and abrasive wear.



(a)  
(b)

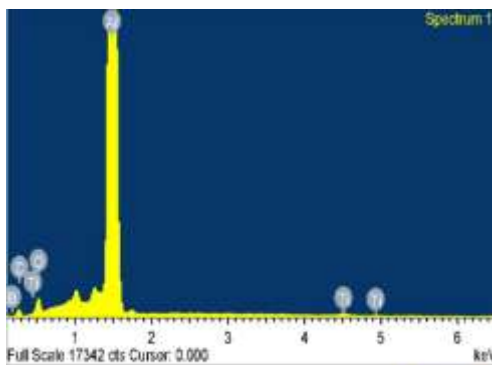
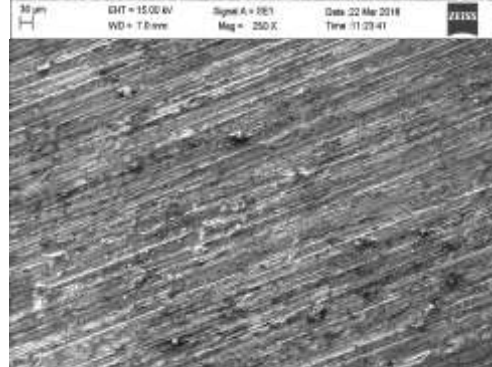
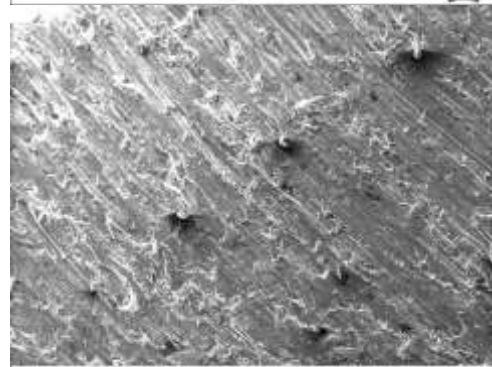
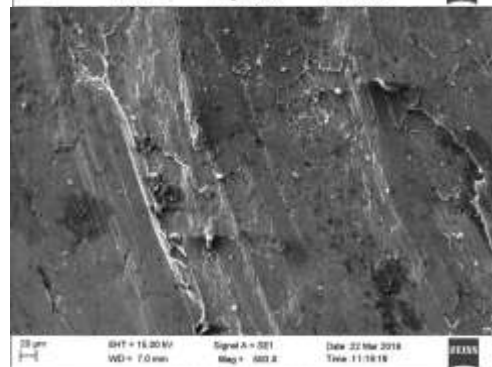
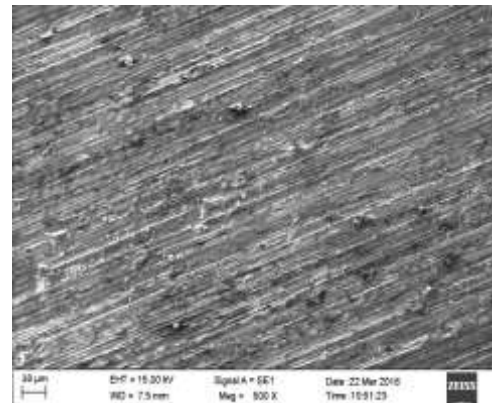


(c) (d)  
**Fig. 4** SEM Photomicrographs of AA6061-B<sub>4</sub>C Composites. (a) 1% B<sub>4</sub>C; (b) 2% B<sub>4</sub>C; (c) 3% B<sub>4</sub>C; (d) 4% B<sub>4</sub>C.

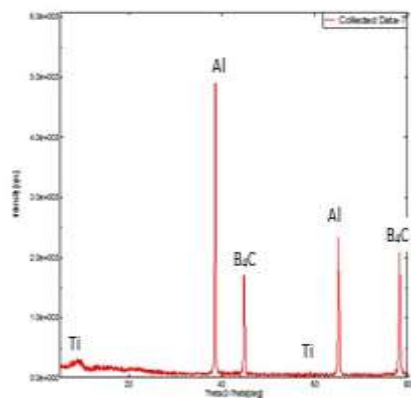


(a) (b)

**Fig. 5** SEM Photomicrographs of AA6061-B<sub>4</sub>C Composites. (a) Micrographs of Ti-rich particles on B<sub>4</sub>C; (b) the enlarged view of Ti-rich particles on B<sub>4</sub>C.



OXFORD  
 INSTRUMENTS  
 The Business of Science



(a) (b)

**Fig. 6** (a) EDAX analysis of AA6061- 4% B<sub>4</sub>C; (b) XRD pattern of AA6061- 4% B<sub>4</sub>C.

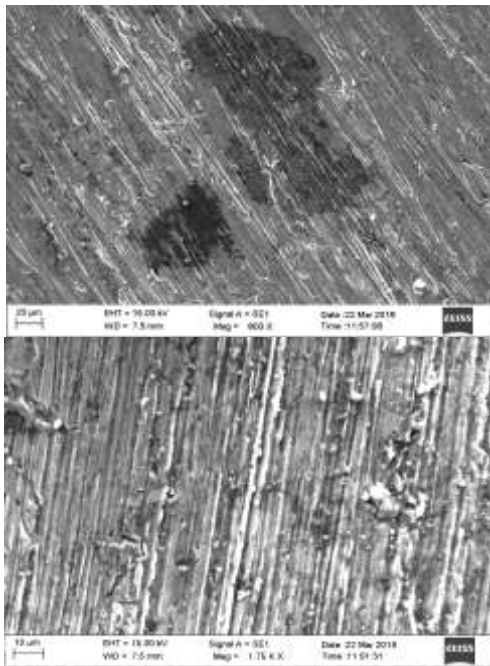


**Fig. 7** SEM Photomicrographs of worn surface at constant sliding speed of 0.9 m/s and constant sliding distance of 282.7m.

#### ACKNOWLEDGEMENTS

The authors acknowledge the R&D Centre, Department of Mechanical Engineering, SJM Institute of Technology, Chitradurga, Vision Group on Science and Technology, Government of Karnataka (K-FIST Level-1 Grant) and Visvesvaraya Technological University (Research Grant) Belagavi, to provide the experimental facilities to carry out the research work. The authors are greatly thankful to Mr. Mahaboob Basha, R & D department for their technical support offered to execute the research work

#### REFERENCES

- [1]. Feng YC, Geng L, Zheng PQ, Zheng ZZ, Wang GS. Fabrication and Characteristic of Al-based hybrid composite reinforced with tungsten oxid particle and aluminium borate whisker by squeeze casting, *Mater Des*, 29, 2008, 2023-6.
- [2]. Kerti I, Toptan F. Microstructural variation in cast B<sub>4</sub>C- reinforced Aluminium matrix composites (AMCs). *Mater Lett*, 62, 2008, 1215-8.
- [3]. Hashim J., Looney L., Hashmi M.S.J., Metal matrix composites: Production by stir casting Method, *Journal of Material Processing and Technology*, 92, 1999, 17.
- [4]. K. Kalaiselvan, N. Murugan, Siva Parameswaran, Production and characterization of AA6061-B<sub>4</sub>C stir cast composites, *Material & Design*, 32, 7, 2011, 4004-4009.
- [5]. Topton F, Kilicarlan A, Cigdem M, Kerti I. Processing and microstructural characterization of

- AA1070 and AA6063 matrix B<sub>4</sub>C reinforced composites. *Material Design*, 31, 2010, S87-91.
- [6]. Kennedy, A.R, Brampton, B. The reactive wetting and incorporation of B<sub>4</sub>C particles into molten aluminium. *Scripta Materialia*, 44, 2001, 1077-1082.
- [7]. Kennedy, A.R. The microstructure and mechanical properties of Al-Si- B<sub>4</sub>C metal matrix composites. *Journal of Material Science*, 37, 2010, 317-323.
- [8]. Topton F, Kilicarlan A, Cigdem M, Kerti I. Processing and microstructural characterization of AA1070 and AA6063 matrix B<sub>4</sub>C reinforced composites, *Material Design*, 31, 2010, 87-91.
- [9]. M. Yandouzi a, A.J. Bottger, R.W.A. Hendrikx, M. Brochu, P. Richer, A. Charest, B. Jodoin, Microstructure and mechanical properties of B<sub>4</sub>C reinforced Al- based matrix composites coatings deposited by CGDS and PGDS process, *Surface & Coating Technology*, 205, 2010, 2234-2246.
- [10]. Marianna Kouzeli, Christopher San Marchi, Andreas Mortensen, Effect of reaction on the tensile behaviour of infiltrated boron carbide aluminium composites, *Materials Science and Engineering*, A337, 2002, 264-273.
- [11]. Ali Yazdani and Salahinejad E, Evolution of Reinforcement distribution in Al- B<sub>4</sub>C composites during accumulative bonding, *Materials & Design*, 2011, 3137-3142.
- [12]. Lashgari H R, Zangeneh S H, Shamir H, Saghafi M, Emamy M. Heat treatment effect on the microstructure tensile properties and dry sliding wear behaviour of AA356-10% B<sub>4</sub>C castcomposites. *Material Design*, 32, 2011, 3263-3271.
- [13]. E. Mohammad Sharifi, F. Karimzadeh, M. H. Enayati, Fabrication and evaluation of mechanical and tribological properties of B<sub>4</sub>C reinforced aluminium matrix nano composites. *Material and Design*, 32, 2011, 3263-3271.
- [14]. G. Straffelini, M. Pellizzari, A. Molinari, Influence of load and temperature on Dry sliding Behaviour of Al- Based Metal matrix composites against friction material, *Wear*, 256, 2004, 754-763.
- [15]. Francois Thevenot, Boron carbide a comprehensive review, *Journal of European ceramic society*, 1990, 205-225.
- [16]. Lembit kommel, Eduard Kimmari, Boron Carbide Based Composite manufacturing and recycling features, *Journal of material science*, 2006, 48-52.
- [17]. Vladislav Domnich, Sara Reynaud, Richard A. Haber, Manish Chhowalla, Boron carbide: structure, properties, stability under stresses, *Journal of American ceramic society*, 2011, 3605-3628.
- [18]. Kume Y, Kobashi M, Kanetake N, Aluminium Alloys, parts 1 and 2, 2006, 519-521.
- [19]. Kaczmar J W, Pietrzak k, Wlosinski W. The Production and Application of metal matrix, Composite materials, *Journal of Material Processing and Technology*, 2000, 58-67.

- 
- [20]. Kouzeli M, Mortensen A, Size dependent Strengthening in particle reinforce Aluminium, *Acta Mater*, 2002, 30-51.
- [21]. Surappa M.K. Aluminium matrix composites, Challenges and opportunities, *Sadhana*, 28, part 1 & 2, 319-334.
- [22]. M. A. El Baradie J., Manufacturing aspects of Metal Matrix Composites, *Journal of Material Processing and Technology*, 24, 1990, 261-272.
- [23]. R. Antonio, C. Subramanian, Wear mechanism map for aluminium alloys, *Scripta Metall*, 22, 1988, 809-814.
- [24]. J. Zhang, A.T. Alpas, Transition between mild and severe wear in aluminium alloys, *Acta mater*, 45, 1997, 513-528.
- [25]. D.M. Aylor, (*Metal Handbooks*, 1982), ASM Metal Park, Ohio, 859-863.
- [26]. Saha P.K. Aluminium extrusion technology, ASM International, 2000.
- [27]. D. M. Stefanescu, *Metals Handbook*, ASM. Ohio, 15, 1998, 105-108.
- [28]. C. A. Smith, Discontinuous reinforcements for metal matrix composites, (*ASM Handbook*, 2010), 21, composites, ASM International.
- [29]. ASTM standard E8. Standard Test Method for Tension testing of metallic materials. West Conshohocken, USA, ASTM International, 2004.
- [30]. ASTM standards, G99-90, Standard Test Method for Wear testing with Pin-On Disc apparatus. (ASTM, 1993), 1-5.